HHS Public Access

Sleep spindle detection: crowdsourcing and evaluating performance of experts, non-experts, and automated methods

Simon C. Warby[1], **Sabrina L. Wendt**[1,2], **Peter Welinder**[3], **Emil G.S. Munk**[1,2], **Oscar Carrillo**[1], **Helge B.D. Sorensen**[4], **Poul Jennum**[2], **Paul E. Peppard**[5], **Pietro Perona**[3], and **Emmanuel Mignot**[1]

[1]Center for Sleep Science and Medicine, Stanford University, California, USA

[2]Danish Center for Sleep Medicine, Glostrup University Hospital, Glostrup, Denmark

[3]Computational Vision Laboratory, California Institute of Technology, Pasadena, California, USA

[4]Dept. of Electrical Engineering, Technical University of Denmark, Kongens Lyngby, Denmark

[5]Department of Population Health Sciences, University of Wisconsin-Madison, Madison, Wisconsin, USA

Abstract

Sleep spindles are discrete, intermittent patterns of brain activity that arise as a result of interactions of several circuits in the brain. Increasingly, these oscillations are of biological and clinical interest because of their role in development, learning, and neurological disorders. We used an internet interface to 'crowdsource' spindle identification from human experts and non-experts, and compared performance with 6 automated detection algorithms in middle-to-older aged subjects from the general population. We also developed a method for forming group consensus, and refined methods of evaluating the performance of event detectors in physiological data such as polysomnography. Compared to the gold standard, the highest performance was by individual experts and the non-expert group consensus, followed by automated spindle detectors. Crowdsourcing the scoring of sleep data is an efficient method to collect large datasets, even for difficult tasks such as spindle identification. Further refinements to automated sleep spindle algorithms are needed for middle-to-older aged subjects.

Keywords

Sleep EEG; electroencephalography; PSG; polysomnography; Performance evaluation; Benchmarking; Reliability; Validity; Agreement; Sensitivity; Specificity; Precision; Recall; Signal

analysis; Pattern recognition; Event detection; EEG microarchitecture; EEG features; Sleep Spindles

INTRODUCTION

Sleep spindles are measured by electroencephalography (EEG) as brief distinct bursts of activity in the sigma frequency range (11–16 Hz). They have a characteristic waxing and waning shape, and are a key EEG feature used during sleep scoring to define non-REM stage 2 (N2) sleep[1]. Sleep spindle characteristics such as density (events/min), amplitude or duration are very stable from night-to-night for an individual[2, 3], but vary substantially between individuals[4, 5]. Spindle oscillation frequency tends to be slower anteriorly and faster centrally/parietally, suggesting there may be two types of spindles[6]. The formation and frequency of spindles have been used as markers of the developing brain in infants[7] and change over the lifespan[8–10]. They are highly heritable[11, 12], and are believed to play an important functional role in synaptic plasticity and memory consolidation during sleep[13–16].

Sleep spindles are also clinically important because alterations in spindle density are observed in several disorders such as schizophrenia[17, 18], autism[19], epilepsy[20], mental retardation[7], sleep disorders[21–23] and neurodegenerative diseases[24]. These are significant changes, as spindles result from interactions of several regions of the brain, including the thalamic reticular nucleus, thalamocortical relay neurons, the hippocampus, and the cortex[25, 26]. During wake, these same circuits are linked to learning, behavioral arousal, and sensory gating[27]. For this reason, identifying and studying characteristics of spindles may reflect the integrity of these circuits in selected pathologies, and could have diagnostic value as biomarkers.

Sleep spindles have traditionally been identified by visual inspection of the EEG by expert technologists in sleep clinics, who are trained in the interpretation of physiological signals from polysomnography. Visual identification by experts is the gold standard for spindle detection. However, visual identification of spindles is a slow and subjective process, and because of the rapidly growing biological and clinical interest in sleep spindles, several automated methods of spindle detection have been developed to speed up and standardize this process. There are several basic methodological strategies for automated spindle detection, and each has given rise to many closely related spindle detectors.

Schimicek et al. published one of the first automated spindle detectors based on a band-pass filtering and amplitude threshold approach[28]. Today, this method is still the foundation for numerous spindle algorithms used and optimized by different research groups[8, 10, 29–40]. Some algorithms replace the standardized band-pass filter with custom frequency range filters for each subject[41–43]. Another modification is to replace the initial band-pass filtering step by an appropriate wavelet transformation[18, 44]. Other modifications include using the shape of the spindle to determine the beginning and end of the spindle rather than having a signal exceeding a constant threshold for the entire spindle duration[17, 45, 46].

However, the performance of many spindle detection algorithms has not been evaluated rigorously. Due to the difficulty in obtaining a gold standard dataset, algorithm development

and testing is frequently performed on the same data. Datasets are typically small (less than 15 subjects) and very few of these detection algorithms have been cross-validated or evaluated in more than one dataset. Furthermore, many of these detectors are designed for use with EEG data from young adults. Spindle identification becomes a more difficult task in older subjects because spindle density, amplitude and duration decrease with age[8, 10]. Although there has been some testing of automated detectors in young adults, the performance of these detectors in older subjects is unclear.

The purpose of this study was to evaluate the performance of spindle identification by trained experts, non-experts, and automated spindle-detection algorithms. To evaluate performance, we compared the spindle detection of each scorer or group consensus to a gold standard dataset. We generated the gold standard data from the group consensus of 24 experts, who visually scored sleep spindles in the stage N2 sleep EEG from 110 subjects from the general population. In order to collect this large dataset we crowdsourced the spindle scoring using an internet interface. This allowed trained experts at multiple sleep clinics to participate. In addition, we used the same interface to collect data from of 114 non-experts, to determine how well they could perform on this skilled task. We developed a simple method for establishing group consensus, and made refinements to the performance evaluation of event-detectors for polysomnography data. Finally, one important goal of this study was to determine in an unbiased manner which of 6 previously published automated spindle detection algorithms had the best performance in our EEG data from older subjects. Overall, spindle detection performance was highest in individual experts and the non-expert group consensus, followed by all automated detection methods we tested.

RESULTS

The EEG data[47] from C3-M2 of 110 healthy subjects was divided into 25 second epochs and in total, 24 experts viewed 10,613 epochs, and 114 non-experts viewed 21,499 epochs for a combined total of 32,112 epoch views. Collection of the expert data took more than 10 months. Collection of the non-expert data took less than 4 days.

Generation of the Gold Standard

The gold standard was established from the expert scorers using the group consensus rule (Supplementary Fig. 1). Each expert viewed a mean of 442 epochs (Fig. 1a). Each of the 2,000 epochs in the dataset was viewed by a mean of 5.3 experts. More than 87 % of the data was viewed by at least 4 experts (Fig. 1b).

The amount of consensus of the expert group is determined by the 'threshold for expert group consensus' (T_{egc}; see methods). To establish the gold standard dataset, we used a T_{egc} of 0.25. This value was used because it is the T_{egc} at which the mean individual expert performance is maximized, and the standard deviation of the mean individual expert performance is minimized (Fig. 1c). We also visually inspected the resulting dataset at various threshold values and found that $T_{egc} = 0.25$ captured the diversity of spindle morphologies with acceptable quality. Below $T_{egc} = 0.25$, there was a large increase in the number of spindles (Fig. 1d), mostly of questionable quality. At $T_{egc} = 0.25$, there were

1987 spindles in the expert group consensus (Fig. 1e). From this point, we refer to the expert group consensus data at T_{egc}= 0.25 as the 'gold standard'.

Performance of Individual Experts

In a by-event analysis against the gold standard, the mean F_1-score performance of individual experts was 0.75±0.06. In the by-sample analysis, the mean F_1-score (0.69±0.06) and Cohen's Kappa score (0.68±0.06, Supplementary Table 1) also indicate good agreement between individual experts and the gold standard, and low variability between experts. From the precision-recall plot, the performance of the individual experts is consistently high, although as expected, some experts emphasize high precision (i.e. greater positive predictive value in identifying spindles) at the expense of recall (i.e. spindle-detection sensitivity), and vice-versa (Fig. 1f).

However, the individual experts are being compared to a gold standard to which their scorings belong, giving them an advantage in the performance evaluation. To control for this, we also compared the individual experts against an expert group consensus in which they did not contribute spindle scoring (Fig. 1f; Supplementary Table 2). The mean F_1-score in the by-event analysis of individual experts after this correction was 0.67±0.07.

Gold Standard - Sleep Spindle Characteristics

More than 70% of all spindles in the gold standard dataset were between 0.5 and 1 second in duration (Fig. 2a, Supplementary Table 3). However, in contrast to the American Academy of Sleep Medicine (AASM) criteria for a lower threshold of 0.5 seconds,[1] we allowed a lower duration threshold of 0.3 seconds, and found 14% of spindles identified by experts fell in the 0.3–0.5 second duration range. We did not find any differences in spindle characteristics of spindles <0.5 seconds versus spindles >0.5 seconds; oscillation frequency was not significantly different, and a weak positive linear correlation between duration and maximum peak-to-peak amplitude was consistent for spindles of all durations. We speculate that spindles 0.5 seconds may be a good criteria for defining N2 sleep, but spindles <0.5 seconds may have the same neurophysiological basis, and are therefore of interest. As well, only 15% of identified spindles had a duration > 1 second. The oscillation frequency of spindles varied from 10.5–16.1 Hz, with a mean of 13.3±1.0 Hz although slightly skewed towards higher frequencies around 14 Hz (Fig. 2b). The mean maximum peak-to-peak amplitude of spindles was 27±11 μV (Fig. 2c), indicating that the majority of spindles in this older cohort of subjects were of moderate-to-low amplitude. The mean percent-to-peak amplitude was 49±21% (i.e. very near the center of the spindle), indicating that on average, spindles tend to have a symmetrical waxing and waning profile (Fig. 2d).

In the gold standard dataset, spindle density was variable between the 110 subjects but had a mean density of 2.3±2.0 spindles/min (Fig. 2e). Consistent with previous reports, subject age was negatively correlated with spindle density (Fig. 2f)[8, 9, 48]. The mean maximum amplitude of spindles was significantly greater in females than males (Fig. 2g), and was negatively correlated with subject age (Fig. 2h). Spindle oscillation frequency tended to be negatively correlated with age although it was not statistically significant (R^2 = 0.037, p-value = 0.051). We also found the mean oscillation frequency and duration were

significantly different between subjects (Fig. 2i). Subjects did not have a clear bimodal distribution of spindle oscillation frequencies (Supplementary Fig. 2). This suggests that there are not discrete categories of 'fast' and 'slow' spindles at this central scalp location in older individuals, rather subject differences of 'faster' and 'slower' spindles, which may be the result of trait-like individual variation. We did not find a significant relationship between spindle density or spindle oscillation frequency with gender, body mass index, apnea/hypopnea index, leg-movement index or total sleep time (linear regression p-values >0.05).

Performance of the Non-Expert Group

The 114 non-experts viewed a mean of 189 epochs each (Fig. 3a). The 2,000 epochs in the dataset were viewed by a mean of 10.7 non-experts (Fig. 3b). More than 99% of the data was viewed by 10 or more non-experts.

As a measure of performance, we calculated the precision and recall of individual non-experts and the non-expert group consensus (Fig. 3c). The maximum by-event F_1-score performance of the non-expert group was 0.67 at a threshold (T_{ngc}) of 0.4 (Fig. 3d), although the group performed reasonably well across a range of consensus thresholds (F_1-score > 0.5 for $0.2 \quad T_{ngc} \quad 0.5$). There was a near exponential relationship between the amount of non-expert consensus and the number of spindles identified (Fig. 3e). At $T_{ngc} = 0.4$, the non-expert group identified 1669 spindles (Fig. 3f), but only 1226 of these were correct (precision = 73%). In other words, of the 1987 spindles in the gold standard, the non-expert group correctly identified 1226 (recall = 62%). Further, the by-subject spindle density correlation was very high ($R^2 = 0.815$; Fig. 3g).

For the non-expert group consensus, we did not perform any data cleaning and used data from all non-experts regardless of how many epochs they actually scored for spindles. Approximately 40 % of the recruited non-experts scored very little data (less than 15 epochs per non-expert). In addition, 11 out of the 2,000 epochs in the gold standard were not viewed by any non-experts. These epochs were interpreted as no spindle calls in the analysis of non-experts since we intended for them to be scored. The performance of the non-expert group consensus compared to the gold standard remains high despite these limitations.

Performance of the Automated Detectors

We implemented and tested 6 previously published spindle detection algorithms. The by-event F_1-score of the automated detectors ranged from 0.21 to 0.52. (Table 1; Supplementary Table 1). Each automated detector tended to find a different balance between recall and precision (Fig. 4a). Detector a4 and a5 had the most balanced approaches (similar recall and precision scores), while a5 had the highest overall by-event F_1-score of the automated detectors.

To determine whether automated detection of spindles could be improved by combining different detectors, we applied the group consensus rule to the group of detectors (Fig. 4a). The maximum F_1-score performance of the automated group was obtained at a group consensus of 0.5 (F_1-score = 0.54, Fig. 4b), but was only slightly better than the single best

automated detector. We attempted to further improve the performance by combining the results of automated detectors without success (Supplementary Note).

To measure the inter-detector agreement, we calculated the F_1-score for each detector pair (Table 1). In general, detectors tended to agree with at least one other detector to a greater degree than with the gold standard. However, even detector pairs that were methodologically similar did not have good agreement between them; the mean agreement between a2-a3-a4, which all use RMS and a constant threshold, was F_1-score = 0.21 ± 0.14. The total number of spindles detected by each detector (range 479 – 13,784), the inter-detector true positive spindle count, and the number of spindles detected in common by two detectors varied greatly (Supplementary Table 4).

The by-subject correlation of spindle density between the gold standard and the automated detectors ranged from $R^2 = 0.01$ to 0.38 (Supplementary Fig. 3). We also compared sigma power as an estimate for spindle density in each subject and found that it predicted spindle density slightly better than the best single automated detector, but not better than the group consensus of the automated detectors (Fig. 4c,d,e).

To determine whether we could optimize the automated detectors to improve their performance, we varied their detection parameters to try and maximize their F_1-score against the gold standard (Supplementary Fig. 4). We found that varying the detection parameters could alter the balance between recall and precision, and in the case of some detectors, improve the F_1-score moderately (Supplementary Table 5). However, even with this attempt to over-fit the detector performance to our data, the maximum performance of any one detector was essentially unchanged (a5, maximum F_1-score = 0.53).

Performance Comparison Between Groups

The by-event precision and recall of individual experts, the non-expert group, and the automated detectors were calculated against the gold standard (Fig. 5a). The by-sample performance of all groups was decreased relative to the by-event performance (Supplementary Table 1) due to the relaxed overlap threshold ($T_{overlap}$) we used for the by-event analysis. $T_{overlap}$ is the amount of overlap between an event and a detection that is required for a detected spindle to match a gold standard spindle event and therefore be considered to be a true positive (see methods).

The by-subject estimate of spindle density varied between the detectors (Fig 5b). The majority of automated detectors and the non-expert group tended to overestimate spindle density for each subject relative to the gold standard, leading to higher recall of spindles in the dataset, but lower overall precision. Detector a3 had the highest recall but overestimated spindle density in the dataset by a factor greater than 7 (Supplementary Table 6).

The majority of detectors, as well as the non-expert group had a tendency to underestimate the mean duration of spindles for each subject (Fig. 5c). Overall however, the range of mean spindle durations between detectors was quite small (0.55 – 0.82 seconds), suggesting that the detectors did a reasonable job of estimating average spindle duration (Supplementary Table 7).

For evaluation of performance in the by-event analysis, we have allowed a relaxed $T_{overlap}$ of 0.2. At this level of overlap, all groups perform at or near to their maximum F_1-score, so we did not constrain performance by the overlap threshold (Fig. 5D; Supplementary Note). Finally, we wanted to determine whether the performance of either the automated detectors or the non-expert group could be improved by selecting a different level of expert group consensus for the gold standard. We found that performance could not be improved; each group performed near-maximal against the chosen gold standard of $T_{egc} > 0.25$ (Supplementary Fig. 5).

We also tested the effect of reducing the minimum spindle duration from 0.5 s to 0.3 s on performance of the automated spindle detectors. We found that reducing the duration from 0.5 s to 0.3 s had little impact on performance in 5/6 of the detectors (mean change in F_1-score = −0.03±0.02, t-test p-value = 0.84) and in one detector (a5), resulted in a large increase in performance (F_1-score +0.16). This increase in performance appears to be due to the tendency of this detector to find many spindles of short duration (Fig. 5c) that would be discarded when using a 0.5 s minimum duration criteria. Taken together, the change of minimum duration did not negatively impact the performance of the automated detectors.

DISCUSSION

Individual experts had consistently high by-event performance, and we were able to further eliminate individual errors using the group consensus rule. As a group, the experts produced a high quality gold standard spindle dataset. To our knowledge, this is the largest and most comprehensively scored sleep spindle dataset used for validation of spindle detectors in older adults.

To our surprise, even though the spindle-detection performance of individual non-experts was highly variable and generally poor, the non-expert group consensus performed as well as some individual experts. This was striking, as we made no attempt at cleaning the non-expert dataset through the removal of low quality scores or missing data; rather we collected a large non-expert dataset and let the group consensus dictate performance. Notably, even though 3–4 non-experts scored a lot of data and performed almost randomly (Fig. 3c), the group consensus rule efficiently screened out this bad data. For non-experts, we found that a higher level of group consensus ($T_{ngc} = 0.4$) compared to experts ($T_{egc} = 0.25$) produced the highest overall performance, which is consistent with the lower level of skill in individual non-experts. These results suggest that crowdsourcing scorings from a large group of non-experts is a viable method to generate large datasets of scored EEG events.

Also to our surprise, we found that the automated detectors performed substantially worse than anticipated in our dataset from older subjects. It was originally our goal to demonstrate how well the detectors perform, and identify which detector performed best relative to humans. However, automated detector performance varied substantially between detectors and was always inferior to human experts or the non-expert group. We were able to increase performance somewhat by using a group consensus rule, but improvement was marginal. In our dataset, the correlation between by-subject spindle density and the estimated spindle density from the best automated detector (a5; $R^2 = 0.38$) was worse than relative sigma

power ($R^2 = 0.46$) or the non-expert group ($R^2 = 0.81$). This correlation with human scoring and relative sigma power suggests that for certain purposes, a large group of human non-experts or relative sigma power may be more useful than existing automated spindle detectors at estimating spindle activity at the by-subject level.

We have implemented each detector as closely as possible to how it has been described previously in order to provide independent validation of their performance. We did not modify or optimize the algorithms because if we did not have a gold standard, there is no way to appropriately optimize the detector. This is the normal situation facing a researcher that wishes to implement a spindle detector in a research project. Without a reference gold standard, changes to the algorithm (such as tuning the detection to a specific spindle density) are arbitrary and can introduce a methodological bias.

However, because we have a gold standard, we could also make adjustments to each algorithm to estimate the maximum possible performance in our dataset from middle/older aged subjects. Although these results would be an over-estimate of future performance due to over-fitting, it does give an indication of maximum performance. By adjusting the detection parameters (primarily the amplitude threshold criteria), we could alter the balance of recall and precision for each detector, and in some cases improve F_1-score moderately. However, we did not find significant increases in F_1-score performance overall, and the maximum performance of the detectors remained essentially unchanged (a5, maximum F_1-score= 0.53).

There are several factors that could lead to the poor performance of the automated detectors. First, the mean age of subjects in this study was 57 ± 8 years. Most of these detectors were designed to work in young, healthy subjects, and our performance measurements may not reflect performance in younger subjects. As expected, we find age-related decline in spindle amplitude, which likely impairs the performance of these amplitude-threshold based algorithms, and raises questions about whether this is a flawed methodological approach for detecting spindles in older subjects. As well, some automated methods use very individualized and specific band-pass approaches that require the detection of both 'fast' and 'slow' spindles at a single location on the scalp. Spindles are believed to be local phenomena [49], and topographical differences in spindle frequency are well described [4, 16, 50]. Our data only assessed spindles at C3, and spindles at other scalp locations may have different characteristics. However, we do not find good evidence to support two discrete populations of spindles at the C3 location in older subjects. The oscillation frequency distributions we observed between subjects (Fig. 2b) and within subjects (Fig. 2i; Supplementary Fig. 2) suggest that at C3, subjects have an individualized distribution, often around a single mean oscillation frequency.

In addition, numerous publications describing automated spindle detectors have evaluated performance using specificity (the fraction of true negatives that are truly negative). As spindles are rare events in a large EEG dataset, the uncalibrated specificity measurement will be consistently high (specificity of the automated detectors we tested ranged from 0.81 to 0.99, Supplementary Table 1), and therefore provide an unrealistically positive and not particularly meaningful evaluation of performance. To avoid this pitfall, we have used

evaluation metrics inspired from information retrieval theory (precision, recall and F_1-score) that are more appropriate to the analysis of discrete events in the EEG signal.

Although our results suggest that human spindle identification was superior to existing automated detection algorithms, there are inherent limitations to manually identified spindles. Automated detectors are more reliable, objective and efficient. It is also possible that automated detectors were able to find obscured spindles in the EEG signal that are difficult for the human eye to see. This may be particularly important in other stages of sleep, such as N3, where spindles are more likely to be obscured by slow waves. It is therefore a reasonable goal to try and find an automated detector to replace human scoring.

However, we find that the agreement between the different automated detectors is generally less than their agreement with the gold standard (Table 1, mean F_1-score agreement between detectors = 0.32±0.16). In other words, this suggests that automated methods as a group were not consistent among themselves; they did not find the same 'hidden' spindles. In addition, each detector had a different bias towards precision or recall, resulting in the under- or over-calling spindle density. This is an important consideration when selecting a spindle detector. It will be important to reconcile the differences between human and automatically detected spindles, and the differences between automated detectors, before the automated detectors can be considered the gold standard.

Implementing the previously published spindle detectors was difficult as we found that almost all publications unintentionally misreported, omitted, or were unclear about critical technical details of the detector. (We emphasize that this is a common problem of computational sciences, rather than something unique to these publications[51]). As a result, it was difficult to reproduce the spindle detection algorithm using information from the publication alone. All of the authors of the detectors we tested were extremely cooperative and kindly shared the original algorithm code, or answered our questions on how to implement their detector correctly. However, considering these difficulties and inherent limitations to describing algorithms methods adequately, we strongly recommend that sharing the algorithm code directly should be seen as an essential part of any publication describing event detectors for physiological signals such as sleep polysomnography.

Improvements in automated spindle detectors can be expected when they are designed against large datasets that capture the diversity of spindle characteristics between subjects (including older age and patient populations), follow proper cross-validation techniques, and use appropriate metrics for assessing performance. Further, a more detailed definition of a sleep spindle is needed, and this definition should be based on the biology and neurophysiology of spindle characteristics. For example, our data suggests that the 0.5 second minimum duration for spindles is arbitrary, and shorter spindles with the same characteristics as longer spindles appear to exist. Sleep technicians also frequently rely on spindles being a 'distinct train of waves' that is clearly distinguishable from background; this is a characteristic that is not captured well by current automated detectors. We argue that the most interesting feature of spindles is how distinctly different their bursting activity is from immediate surrounding activity, because of the neurophysiological changes that are required to generate these rapid changes.

In conclusion, our study demonstrates that crowdsourcing experts and non-experts is a viable method for generating a large dataset of EEG event detections. Currently, the spindle detection performance of several automated algorithms was less than expert or non-expert group performance in this challenging dataset from older subjects. We generated spindle identifications across a large number of subjects, and found a large amount of inter-subject variation in spindles. This dataset will serve as an indispensable reference to reflect inter-individual diversity in these traits, and as a platform to develop, improve and evaluate the performance of automated spindle detectors.

ONLINE METHODS

EEG Dataset

The EEG dataset used for spindle identification was extracted from a randomly selected subset of 110 subjects from the Wisconsin Sleep Cohort[47]. From 100 subjects, we randomly selected 230 seconds (~4 minutes) of artifact-free N2 sleep (2 blocks of 115 s, each block divided in 5 consecutive 25 s epochs overlapping 2.5 s, for a total of 10 epochs per subject). In the remaining 10 subjects we randomly selected 2300s (~38 minutes) of N2 sleep (20 blocks of 115 s, each block divided in 5 consecutive 25 s epochs overlapping 2.5 s, for a total of 100 epochs per subject). Epochs containing EEG signal artifacts were discarded after visual inspection. In total, the raw EEG dataset was composed of 2,000 epochs of N2 sleep. The mean age of the 110 subjects was 57 ± 8 years; 53% of the cohort was female. Demographics of the subjects are representative of middle to older-age subjects as in the parent Wisconsin Sleep Cohort, which is a sample of the general population (Supplementary Table 8). All subjects provided written consent, and data collection and usage was approved by the University of Wisconsin-Madison and Stanford University Institutional Review Boards.

Spindle Identification - Data Collection Using an Internet Interface

To collect a large sleep spindle dataset, we developed an internet interface so that identification could be collected remotely from a large group of scorers ('crowdsourced'). The internet interface presented EEG data one epoch at a time and allowed the visual identification of sleep spindles by human scorers. The EEG data was displayed using an epoch length of 25 s to ensure that the entire epoch would fit in a standard size internet browser window, and would not require the scorer to scroll back and forth to view the whole epoch.

The data presented was from a single EEG channel (C3-M2), originally sampled at 100 Hz and filtered using standard clinical procedures (<0.3Hz, >35Hz[1]). Spindle amplitude and frequency is maximal at C3[50]. An example of EEG data presentation using the web interface is shown in Supplementary Figure 6. We were particularly careful to ensure that data was presented in a familiar way for sleep experts (i.e. aspect ratio of the images was maintained, negative voltages were always displayed upward and values ranged from -50 to 50 μV; values out of this range were truncated to either of these limits). A 25 s epoch of EEG was converted to an image of size 900x90 pixels. Vertical gridlines identified 0.5 s increments.

The EEG data was organized in blocks of 5 epochs from one subject, and the blocks of epochs were presented to the human scorers in random order. To minimize edge effects of identifying spindles that fell within an epoch boundary, epoch images were overlapped by 2.5s, so that EEG data that fell at the edge of an epoch in one image would be 2.5s away from the edge in a subsequent image. Any spindle identifications that were falsely split due to epoch boundaries were merged using a simple rule: If the duration of the spindle was less than 0.3s and the adjacent spindle was less than 0.1s away, the two identifications were merged. Following merging spindles that were split by the epoch boundary, any remaining spindle identifications less than 0.3s were discarded. Overall, the merging rule resulted in merging of 6 spindles. Twenty-seven spindles in the gold standard dataset were discarded for being less than 0.3 seconds.

Spindle identification was performed in the interface by drawing a bounding box around spindle events. To indicate scoring certainty in the presence of a spindle, each bounding box had to be labeled with a confidence score: 'Definitely', 'Probably', 'Maybe'/'Guessing'. In cases where no spindle events were detected, scorers were allowed to indicate that they did not detect any spindles in that epoch by checking the 'There are no spindles in the image' checkbox. Scorers were able to go back and review or change their previous spindle identifications within a block of epochs.

Human Non-Expert Scorers

The human non-expert spindle scorers were recruited from the Amazon Mechanical Turk website (https://www.mturk.com/mturk/). The non-experts were paid piece-wise for their work, and were not screened for any experience with sleep or EEG data. Non-experts were instructed to read lay-language instructions on spindle identification (Supplementary Fig. 7) and performed a brief training session (15 epochs) before the actual spindle identification task.

Human Expert Scorers

Registered Polysomnographic Technologists (RPSGTs) were recruited as our expert scorers. These experts were recruited by word-of-mouth and from an advertisement on an online forum. In total, we recruited 24 experts from sleep clinics in the United States and Canada. Experts were instructed to read the same instructions and perform the same training session as non-experts. Experts were either paid piece-wise for the data collection or volunteered their time. The most productive experts received small gifts for their work.

Automated Spindle Detectors

We evaluated the performance of 6 previously published spindle detection algorithms that are commonly used in the research literature. These detectors are labeled as a1[41], a2[17], a3[31], a4[10], a5[18], and a6[45]. These algorithms are similar in their basic methodology, and all but one[18] rely on initial band-pass filtering in the spindle frequency range. We made one change to all of the automated detectors in that we allowed them to detect spindles with durations as short at 0.3 s, since spindles of this duration are included in our gold standard dataset.

We implemented two methods[10, 31] derived from Schimicek[28] since many algorithms are branching off from it (see introduction). The method can briefly be described as band-pass filtering in the spindle frequency range, calculating the root-mean-square (RMS) of the signal in a moving window, and applying a constant threshold based on the amplitude of the RMS signal. Spindles are detected where the RMS exceeds the threshold for a specified minimum duration. The two implementations[10, 31] differ in the frequency range of the band-pass filter, in the time resolution and window size for calculating the RMS, and in the definition of the threshold.

Moreover, we implemented a wavelet based algorithm[18]. First the data is wavelet transformed using a complex morlet wavelet mimicking a spindle shape and frequency content. Afterwards the moving average of the coefficients is calculated and the mean is used to obtain the threshold for spindle detection.

We also implemented an automated detector that uses individual spindle characteristics of each subject prior to detection[41]. For this detector, precise frequency boundaries for slow and fast spindles are first derived from the all night average amplitude spectrum during N2 sleep. We used data from C3 and O1 to determine individual spindle characteristics whereas the original method uses 29 channels. The spectrum is also used to derive the amplitude criteria for spindle detection. After determining these measures, data is band-pass filtered in either of the two bands and subjected to a constant threshold at the corresponding amplitude criteria.

Finally we implemented two methods that use the spindle envelope to find the beginning and the end of a spindle after a part of the signal within these boundaries has exceeded the threshold[17, 45]. One of the methods uses only local minima for boundaries[17] whereas the other method uses local extrema of the signal and its first derivative[45].

Pseudo-code of the different sleep spindle detector algorithms are presented in Supplementary Figure 8 to help the reader understand the details of how each detector works. Some detectors were originally implemented in other programs; for these, we have re-implemented the algorithms in MATLAB, and as such they may be slightly different from the original. In some cases, we confirmed the similarity of the output by running both the original and MATLAB implementation of the detector on the same dataset and comparing the results. Our MATLAB code for each detector is available as Supplementary Software.

Group Consensus Rule

In order to produce a high-quality gold standard dataset, we aggregated the identifications from multiple experts using a group consensus rule. The same group consensus rule is used to find the non-expert group consensus and the automated group consensus. Based on the confidence score provided by the human scorers, we assigned each annotation a weighted value: 1 ('Definitely'), 0.75 ('Probably'), 0.5 ('Maybe'/'Guessing') and 0 (Not Spindle). The automated spindle detections were always given a confidence value of 1. To find the group consensus at the ith sample we took the mean confidence values at the ith sample. To determine whether the group finds a spindle or not at each sample point, the group mean

confidence value must exceed the threshold (T_{gc}). The group consensus can vary from little consensus (gc >~0.0) to perfect agreement of all scorers (where gc = 1). An example of how the group consensus rule is applied for at T_{gc} of 0.25 is provided in Supplementary Figure 1. The group consensus threshold will be referred to as T_{egc} for expert group consensus, T_{ngc} for non-expert group consensus and T_{agc} for automated group consensus. The gold standard is established from the expert group consensus at $T_{egc} = 0.25$. The strength of the group consensus method is that it requires agreement among the scorers and eliminates outlier data. In datasets such as EEG, where events such as spindles only make up a small proportion of the total data, poorly or randomly identifying events is unlikely to be included in the group consensus, as multiple scorers have to make the same identification. Real examples of the consensus in experts, non-experts, and automated detectors are provided in Supplementary Figure 9.

Performance Evaluation

Performance of human scorers or automated detectors was always compared to the gold standard. We define individual spindles in the gold standard dataset to be events (E), while individual spindles identified by humans or detected by automated algorithms to be event detections (D). For event detections in EEG data such as sleep spindles, performance can be assessed in three different data domains, each having a different unit of measurement: by-sample, by-event and by-subject.

The by-sample performance analysis provides the most precise details about actual performance and is equivocally determined. However, since the unit of measurement is a sample point, it can be difficult to interpret the results because spindle events can be composed of variable numbers of samples. By-event performance evaluation is easier to interpret, but difficult to calculate because events and detections are of variable length and can have variable overlap. We will present a set of rules for matching spindle events and detections to accommodate less-than-perfect or multiple overlaps. The by-subject analysis, which summarizes information about each subject (e.g. spindle density) and is the easiest to calculate, does not provide any direct information about the detector's ability to identify the location of spindles in the EEG data.

By-Sample Performance Analysis

In the by-sample analysis, the unit of measurement is digital sample points, which are uniform in length and non-overlapping (i.e. a signal sampled with 100 Hz contains 100 samples per second). Building a classic 2x2 contingency table by calculating the number of true positive (TP), true negative (TN), false positive (FP) and false negative (FN) samples is straightforward (see Definitions, Supplementary Fig. 10). However, since spindle events in EEG are relatively rare, the vast majority of sample points in the data will be TN, regardless of how well a detector performs. For this reason, uncalibrated 'specificity' does not provide a meaningful assessment of performance. Instead, 'recall' and 'precision' provide a more useful assessment of performance and are calculated as:

$$recall = \frac{TP}{TP+FN} = fraction\ of\ true\ spindle\ events\ found$$
$$precision = \frac{TP}{TP+FP} = fraction\ of\ detections\ that\ are\ correct$$

Recall is the same as 'sensitivity' or 1- 'miss rate'. Precision is the same as positive predictive value (PPV), 'selectivity', or 'hit rate'. Although the terms sensitivity and positive predictive value are more commonly used for diagnostic tests, the spindle detection task is more similar to the task of information retrieval, where precision and recall are more widely used. Precision and recall both can vary from 0 to a maximum of 1; a perfect scorer would fall in the top right corner of a precision-recall plot.

These two measures can be combined to obtain a single F_1-score of agreement, which is the harmonic mean of precision and recall, ranging from 0 (no agreement with the standard) to 1 (perfect agreement with the standard).

$$F_1 - score = 2 * \frac{Precision * recall}{Precision + recall}$$

In the by-sample analysis it is also possible to calculate additional coefficients summarizing the performance using the contingency table, such as Cohen's Kappa or Matthews Correlation Coefficient, which correct for the large bias toward TN in the sparse EEG dataset. We found that these coefficients gave similar performance results to the F_1-score. The by-sample analysis penalizes detections that do not align perfectly with the matching event and therefore provides the most detailed and rigorous assessment of detector performance.

By-Event Performance Analysis

In the event-by-event analysis, the unit of measurement is the single sleep spindle, which can be variable in length. By-event scoring is classifying each spindle event and detection into a contingency table of TP, FP, and FN. Since non-spindle events (TN) are also variable in length and are not meaningful, they are not counted in the by-event analysis. As with the by-sample analysis, the by-event performance measures are recall, precision and F_1-score.

To resolve the less-than-perfect overlap and multiple overlap problems between spindle events and detections, a matching procedure is used to establish event-detection (ED) pairs. Multiple overlaps are not allowed; only one D can be matched with one E. The best match is determined by the ED pair with the maximum intersection/union score (max O_{ED}) that exceeds the overlap threshold ($T_{overlap}$) which specifies how much overlap is required to match an E and D as an ED pair. In case of an exact tie in max O_{ED} scores, the temporally first ED pair is selected as the ED match. At the end of the matching procedure all matched ED pairs are TP, all unmatched E's are FN, and all unmatched D's are FP.

$$O_{ED} = \frac{E \cap D}{E \cup D}$$

$$O_{ED} > \mathrm{T}_{overlap} \xrightarrow{yields} TP$$

Pseudo-code explaining the details of the event matching and scoring rule is presented in Supplementary Figure 11. Depending on the required $T_{overlap}$, the by-event analysis is less strict than the by-sample analysis, as it allows the spindle events to be detected with less-than-perfect overlap. Throughout this study, we used a relaxed overlap threshold value of $T_{overlap} = 0.2$, unless stated otherwise. Since it provides the most intuitive results, the bulk of our performance evaluation for the detectors is presented using the by-event analysis.

By-Subject Performance Analysis

The unit of measurement in the by-subject analysis is the sleeping individual. Performance is based on how the aggregate measure of all spindle detected events for a sleeping individual (total spindle count, spindle density, mean spindle duration, etc.) correlates between the gold standard and scorer/detector estimate (linear model R^2). The by-subject analysis is useful to investigate the superficial performance of the detection method. If a detection method performs poorly in the by-subject analysis it will also perform poorly in the by-sample and by-event analysis. However, the opposite is not necessarily true. The by-subject analysis does not directly provide information on how spindle detections match with the actual spindle events in the EEG time series.

We also calculate mean relative sigma power of the EEG signal in the dataset to estimate spindle activity at the by-subject level. The relative sigma power is estimated in 2 second windows with 50 % overlap in all continuous segments of spindle scored data in each subject. The windows are Hanning corrected before being fast Fourier transformed. The relative sigma power is calculated as the absolute sigma power (sum between 11 and 16 Hz) divided by the difference in total power (sum between 0 and 30 Hz) and absolute sigma power. The relative sigma power for all windows is averaged to derive the mean relative sigma power per subject. Note that relative sigma power was only calculated on portions of EEG that are included in the dataset (not all N2 or all NREM).

Handling of Missing Data

When comparing an individual expert or non-expert to the gold standard, only the subset of the data viewed by the scorer is used for performance evaluation; an individual scorer is not evaluated on EEG data they did not view. Average group performance is simply the mean performance of all individuals in the group. Average group performance is therefore different than the performance of the group consensus, in which the single group consensus is formed using the group consensus rule, and then performance of this consensus is made against the gold standard. Note that any missing data at the group level (i.e. 11 epochs that were not viewed by any non-experts), were used in the group consensus performance evaluation and interpreted as no spindle identifications. This distinction was made to keep the gold standard dataset consistent in size, since we intended to have non-expert coverage of the entire dataset.

Spindle Characterization

Identified spindles can be described by several characteristics including: oscillation frequency, maximum peak-to-peak amplitude, and spindle symmetry. After band-pass filtering the EEG containing the spindle between 11–16 Hz using a 253th order equiripple FIR filter with stop-band attenuations of 10^{-4} at 10 and 17 Hz, the oscillation frequency (Hz) is calculated by dividing the sampling frequency by the mean inter-peak interval within the spindle (maxima to maxima intervals and minima to minima intervals, ignoring minor fluctuations). The maximum peak-to-peak amplitude (μV) is the maximum difference between adjacent local maxima and minima (peaks) within the 11–16 Hz filtered spindle event. The spindle symmetry relates to the symmetry/skewedness of the spindle's waxing and waning shape and is calculated by identifying the percentile within a spindle duration where the maximum peak-to-peak amplitude occurs; a spindle with the maximum amplitude exactly in the middle of the spindle duration would have a symmetry score of 0.5. Spindle characterization was performed on spindles in the gold standard (Fig. 2), as well as spindles identified by automated detectors (Supplementary Note; Supplementary Fig. 11 &12).

Statistical Analysis

Statistical analysis (two-tailed t-test, one-way ANOVA or linear regression as appropriate) was performed using R (http://www.r-project.org/). The significance threshold used was alpha = 0.05. Averages are shown as means ± standard deviations (SD). Histograms are plotted using the following conventions: If the data is non-continuous, the tick is centered in the bar. If the data is continuous, the bars are justified left (i.e. the value at the tick belongs in the bar to the right of the tick).

Supplementary Material

Refer to Web version on PubMed Central for supplementary material.

Acknowledgments

References

1. Iber, C.; Ancoli-Israel, S.; Chesson, A.; Quan, SF. AASM Manual for the Scoring of Sleep and Associated Events. 2007.

2. Silverstein LD, Levy CM. The stability of the sigma sleep spindle. Electroencephalogr Clin Neurophysiol. 1976; 40:666–670. [PubMed: 57053]

3. Tan X, Campbell IG, Feinberg I. Internight reliability and benchmark values for computer analyses of non-rapid eye movement (NREM) and REM EEG in normal young adult and elderly subjects. Clin Neurophysiol. 2001; 112:1540–1552. [PubMed: 11459695]

4. Werth E, Achermann P, Dijk DJ, Borbély AA. Spindle frequency activity in the sleep EEG: individual differences and topographic distribution. Electroencephalogr Clin Neurophysiol. 1997; 103:535–542. [PubMed: 9402884]

5. De Gennaro L, Ferrara M, Vecchio F, Curcio G, Bertini M. An electroencephalographic fingerprint of human sleep. Neuroimage. 2005; 26:114–122. [PubMed: 15862211]

6. De Gennaro L, Ferrara M. Sleep spindles: an overview. Sleep Med Rev. 2003; 7:423–440. [PubMed: 14573378]

7. Shibagaki M, Kiyono S, Watanabe K. Spindle evolution in normal and mentally retarded children: a review. Sleep. 1982; 5:47–57. [PubMed: 7071451]

8. Crowley K, Trinder J, Kim Y, Carrington M, Colrain IM. The effects of normal aging on sleep spindle and K-complex production. Clin Neurophysiol. 2002; 113:1615–1622. [PubMed: 12350438]

9. Nicolas A, Petit D, Rompré S, Montplaisir J. Sleep spindle characteristics in healthy subjects of different age groups. Clin Neurophysiol. 2001; 112:521–527. [PubMed: 11222974]

10. Martin N, et al. Topography of age-related changes in sleep spindles. Neurobiol Aging. 2013; 34:468–476. [PubMed: 22809452]

11. De Gennaro L, et al. The electroencephalographic fingerprint of sleep is genetically determined: a twin study. Ann Neurol. 2008; 64:455–460. [PubMed: 18688819]

12. Ambrosius U, et al. Heritability of sleep electroencephalogram. Biol Psychiatry. 2008; 64:344–348. [PubMed: 18405882]

13. Fogel SM, Smith CT. The function of the sleep spindle: a physiological index of intelligence and a mechanism for sleep-dependent memory consolidation. Neurosci Biobehav Rev. 2011; 35:1154–1165. [PubMed: 21167865]

14. Walker MP. The role of sleep in cognition and emotion. Ann N Y Acad Sci. 2009; 1156:168–197. [PubMed: 19338508]

15. Diekelmann S, Born J. The memory function of sleep. Nat Rev Neurosci. 2010; 11:114–126. [PubMed: 20046194]

16. Barakat M, et al. Fast and slow spindle involvement in the consolidation of a new motor sequence. Behav Brain Res. 2011; 217:117–121. [PubMed: 20974183]

17. Ferrarelli F, et al. Reduced sleep spindle activity in schizophrenia patients. Am J Psychiatry. 2007; 164:483–492. [PubMed: 17329474]

18. Wamsley EJ, et al. Reduced sleep spindles and spindle coherence in schizophrenia: mechanisms of impaired memory consolidation? Biol Psychiatry. 2012; 71:154–161. [PubMed: 21967958]

19. Limoges E, Mottron L, Bolduc C, Berthiaume C, Godbout R. Atypical sleep architecture and the autism phenotype. Brain. 2005; 128:1049–1061. [PubMed: 15705609]

20. Myatchin I, Lagae L. Sleep spindle abnormalities in children with generalized spike-wave discharges. Pediatr Neurol. 2007; 36:106–111. [PubMed: 17275662]

21. Montagna P, Gambetti P, Cortelli P, Lugaresi E. Familial and sporadic fatal insomnia. Lancet Neurol. 2003; 2:167–176. [PubMed: 12849238]

22. Espa F, Ondze B, Deglise P, Billiard M, Besset A. Sleep architecture, slow wave activity, and sleep spindles in adult patients with sleepwalking and sleep terrors. Clin Neurophysiol. 2000; 111:929–939. [PubMed: 10802466]

23. Himanen SL, Virkkala J, Huupponen E, Hasan J. Spindle frequency remains slow in sleep apnea patients throughout the night. Sleep Medicine. 2003; 4:229–234. [PubMed: 14592327]

24. Petit D, Gagnon JF, Fantini ML, Ferini-Strambi L, Montplaisir J. Sleep and quantitative EEG in neurodegenerative disorders. J Psychosom Res. 2004; 56:487–496. [PubMed: 15172204]

25. Ferrara M, Moroni F, De Gennaro L, Nobili L. Hippocampal sleep features: relations to human memory function. Frontiers in Neurology. 2012; 3

26. Steriade M. Grouping of brain rhythms in corticothalamic systems. Neuroscience. 2006; 137:1087–1106. [PubMed: 16343791]

27. Vukadinovic Z. Sleep abnormalities in schizophrenia may suggest impaired trans-thalamic cortico-cortical communication: towards a dynamic model of the illness. Eur J Neurosci. 2011; 34:1031–1039. [PubMed: 21895800]

28. Schimicek P, Zeitlhofer J, Anderer P, Saletu B. Automatic sleep-spindle detection procedure: aspects of reliability and validity. Clin Electroencephalogr. 1994; 25:26–29. [PubMed: 8174288]

29. Huupponen E, et al. Optimization of sigma amplitude threshold in sleep spindle detection. J Sleep Res. 2000; 9:327–334. [PubMed: 11386202]

30. Gais S, Mölle M, Helms K, Born J. Learning-dependent increases in sleep spindle density. J Neurosci. 2002; 22:6830–6834. [PubMed: 12151563]

31. Mölle M, Marshall L, Gais S, Born J. Grouping of spindle activity during slow oscillations in human non-rapid eye movement sleep. J Neurosci. 2002; 22:10941–10947. [PubMed: 12486189]

32. Anderer P, et al. An E-health solution for automatic sleep classification according to Rechtschaffen and Kales: validation study of the Somnolyzer 24 x 7 utilizing the Siesta database. Neuropsychobiology. 2005; 51:115–133. [PubMed: 15838184]

33. Schabus M, et al. Sleep spindle-related activity in the human EEG and its relation to general cognitive and learning abilities. Eur J Neurosci. 2006; 23:1738–1746. [PubMed: 16623830]

34. Huupponen E, et al. Development and comparison of four sleep spindle detection methods. Artif Intell Med. 2007; 40:157–170. [PubMed: 17555950]

35. Devuyst S, et al. Automatic sleep spindle detection in patients with sleep disorders. Conf Proc IEEE Eng Med Biol Soc. 2006; 1:3883–3886. [PubMed: 17947058]

36. Barakat M, et al. Sleep spindles predict neural and behavioral changes in motor sequence consolidation. Hum Brain Mapp. 2013; 34:2918–2928. [PubMed: 22674673]

37. Bergmann TO, Molle M, Diedrichs J, Born J, Siebner HR. Sleep spindle-related reactivation of category-specific cortical regions after learning face-scene associations. Neuroimage. 2012; 59:2733–2742. [PubMed: 22037418]

38. Ayoub A, et al. Differential effects on fast and slow spindle activity, and the sleep slow oscillation in humans with carbamazepine and flunarizine to antagonize voltage-dependent na(+) and ca(2+) channel activity. Sleep. 2013; 36:905–911. [PubMed: 23729934]

39. Ray LB, Fogel SM, Smith CT, Peters KR. Validating an automated sleep spindle detection algorithm using an individualized approach. J Sleep Res. 2010; 19:374–378. [PubMed: 20149067]

40. Schabus M, et al. Hemodynamic cerebral correlates of sleep spindles during human non-rapid eye movement sleep. Proc Natl Acad Sci US A. 2007; 104:13164–13169.

41. Bódizs R, Körmendi J, Rigó P, Lázár AS. The individual adjustment method of sleep spindle analysis: methodological improvements and roots in the fingerprint paradigm. J Neurosci Methods. 2009; 178:205–213. [PubMed: 19061915]

42. Ruch S, et al. Sleep stage II contributes to the consolidation of declarative memories. Neuropsychologia. 2012; 50:2389–2396. [PubMed: 22750121]

43. Bódizs R, Gombos F, Kovács I. Sleep EEG fingerprints reveal accelerated thalamocortical oscillatory dynamics in Williams syndrome. Res Dev Disabil. 2012; 33:153–164. [PubMed: 22093660]

44. Sitnikova E, Hramov AE, Koronovsky AA, van Luijtelaar G. Sleep spindles and spike-wave discharges in EEG: Their generic features, similarities and distinctions disclosed with Fourier transform and continuous wavelet analysis. J Neurosci Methods. 2009; 180:304–316. [PubMed: 19383511]

45. Wendt SL, et al. Validation of a novel automatic sleep spindle detector with high performance during sleep in middle aged subjects. Conf Proc IEEE Eng Med Biol Soc. 2012; 2012:4250–4253. [PubMed: 23366866]

46. Plante DT, et al. Topographic and sex-related differences in sleep spindles in major depressive disorder: a high-density EEG investigation. J Affect Disord. 2013; 146:120–125. [PubMed: 22974470]

47. Peppard PE, et al. Increased Prevalence of Sleep-Disordered Breathing in Adults. Am J Epidemiol. 2013; 177:1006–1014. [PubMed: 23589584]

48. Feinberg I, Koresko RL, Heller N. EEG sleep patterns as a function of normal and pathological aging in man. J Psychiatr Res. 1967; 5:107–144. [PubMed: 6056816]

49. Nir Y, et al. Regional slow waves and spindles in human sleep. Neuron. 2011; 70:153–169. [PubMed: 21482364]

50. McCormick L, Nielsen T, Nicolas A, Ptito M, Montplaisir J. Topographical distribution of spindles and K-complexes in normal subjects. Sleep. 1997; 20:939–941. [PubMed: 9456457]

51. Donoho DL. An invitation to reproducible computational research. Biostatistics (Oxford, England). 2010; 11:385–388.
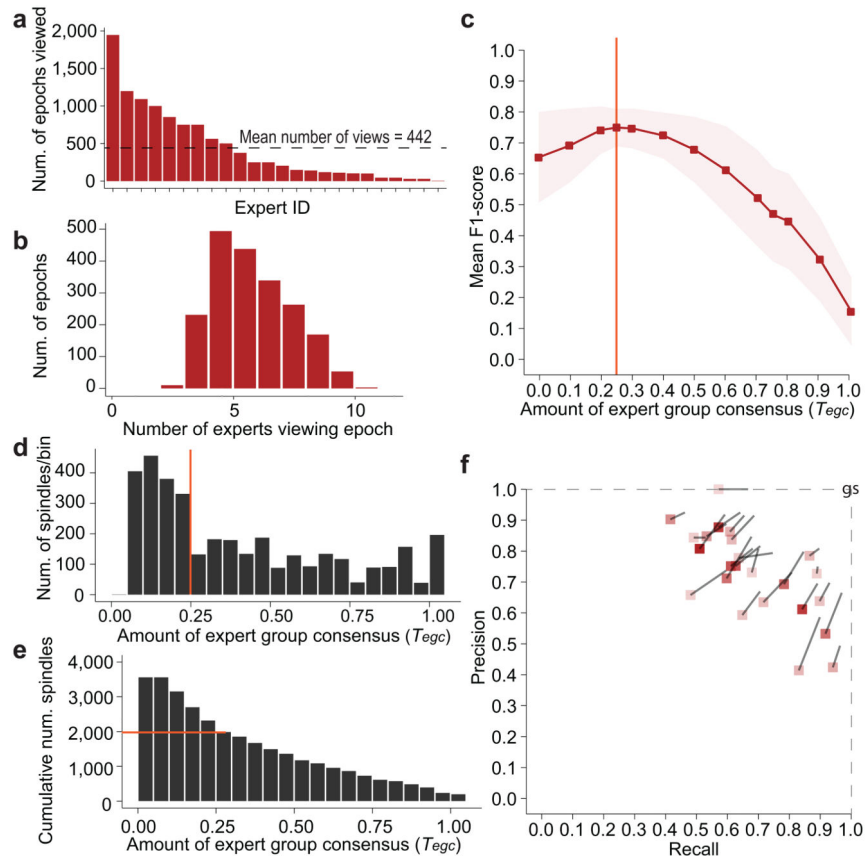
Figure 1.

Generation of the gold standard and spindle detection performance of individual experts. (a) Histogram of the number of epochs viewed by 24 expert scorers. Each bin represents one expert, and they are arranged in descending order. (b) Histogram of the number of times epochs were viewed by a specific number of experts. (c) Mean by-event performance (F_1-score) of individual experts (shading is standard deviation) at varying thresholds of consensus. Average performance was maximized at $T_{egc} = 0.25$, and this level of group consensus was used to generate the gold standard expert dataset. (d) Number of spindles found at each T_{egc} threshold bin. Vertical line indicates optimal performance at $T_{egc} = 0.25$. (e) Cumulative number of spindles over the T_{egc} range. Horizontal line indicates the expert group identified 1987 spindles at $T_{egc} = 0.25$. (f) Precision-recall plot of individual expert performance. Each square is one expert; the intensity of the color is scaled according to how many epochs each expert viewed. The darkest squares are the experts that saw the most data. The line connected to each square indicates the decrease in performance in the leave-one-out analysis that excludes the individual from the expert group consensus to correct for reporting bias. The position of the square indicates the performance after correction.
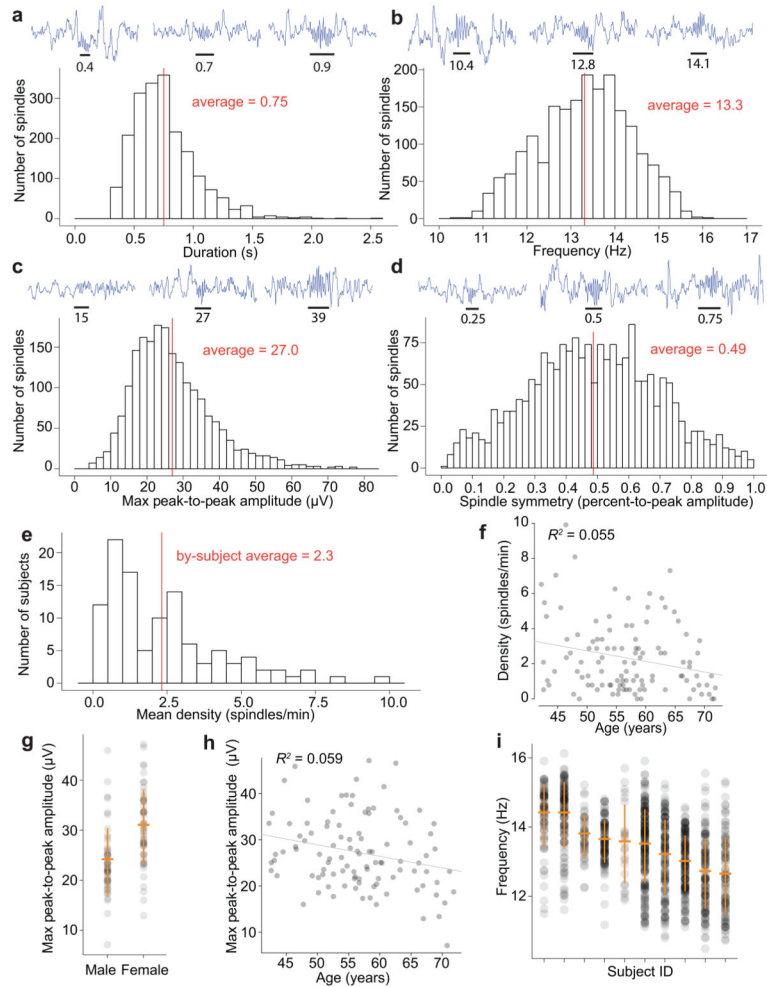
Figure 2.
By-event and by-subject characteristics of 1,988 spindles in the gold standard dataset. (a) Duration. (b) Frequency. (c) Maximum peak-to-peak amplitude in the 11–16 Hz band. (d) Symmetry, measured as location of the maximum peak-to-peak amplitude relative to the length of the spindle. Example spindles for each characteristic is provided above the histogram. Black bars indicate spindle identification. (e) Spindle density in the 110 subjects. (f) Correlation between spindle density and subject age ($R^2 = 0.055$, p-value = 0.013). (g) Mean maximum peak-to-peak amplitude of spindles in females versus males (t-test p-value = 3.03e^{-6}). (h) Correlation between maximum peak-to-peak amplitude and subject age ($R^2 = 0.059$. p-value = 0.016). (i) Spindle oscillation frequency between subjects (ANOVA p-value = 9.93e^{-70}), ordered by descending mean frequency.
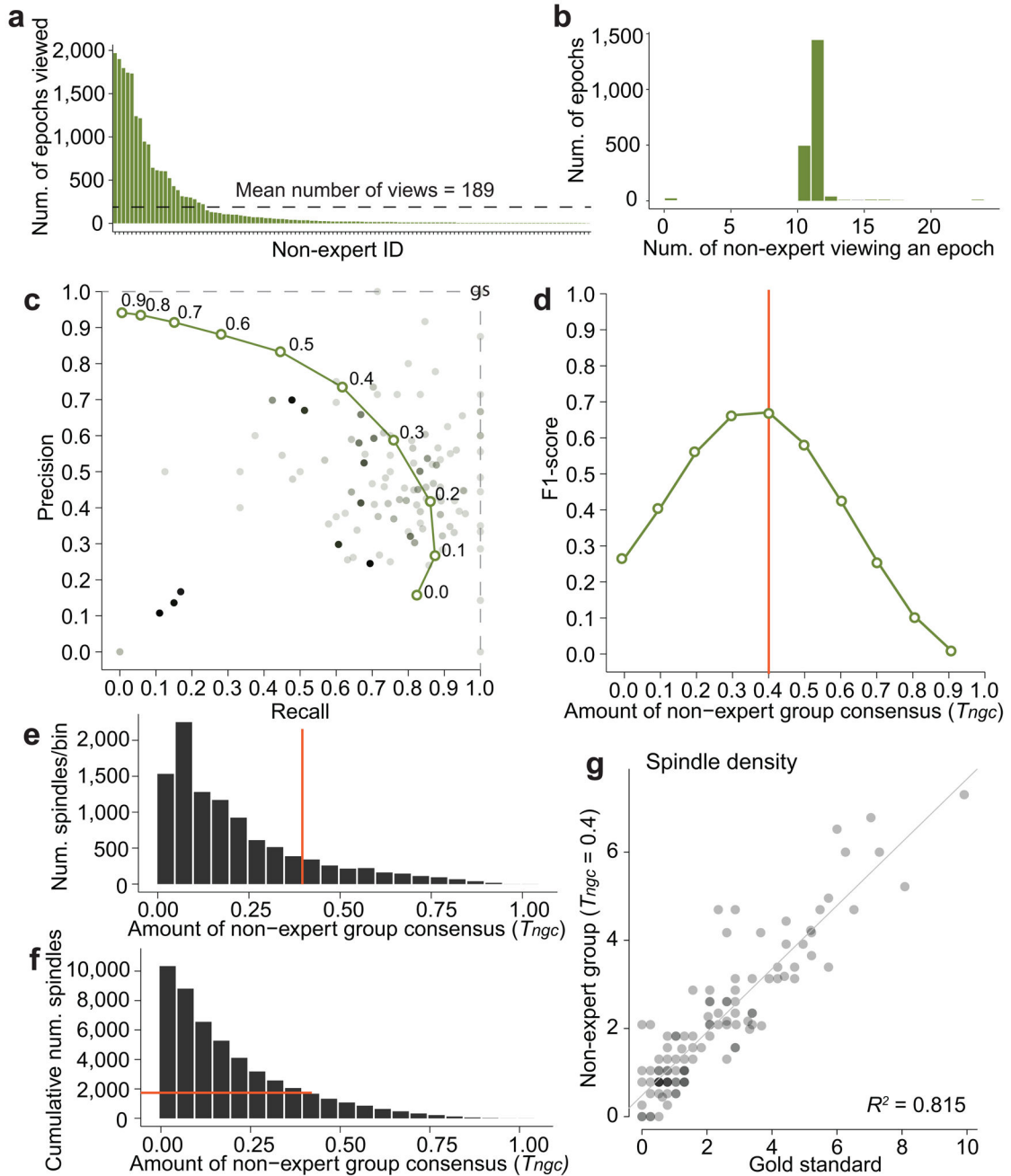
Figure 3.

Consensus and performance of the non-expert group for spindle detection. (a) Histogram of the number of epochs viewed by each of 114 non-expert scorers. Each bin represents one non-expert, and they are arranged in descending order. (b) Histogram of the number of times epochs are viewed by a specific number of non-experts. (c) By-event precision-recall plot of non-expert performance. Each circle is one non-expert; non-experts that viewed the most data are the darkest circles. Non-expert group consensus is plotted as a green line; performance at each consensus threshold (0–0.9) is indicated with a green circle. Performance of the group consensus is remarkably good, despite individuals with very low

performance (bottom left). (d) F_1-score performance of the non-expert group consensus at different consensus thresholds (T_{ngc}) in the by-event analysis. Optimal performance was $T_{ngc} = 0.4$. (e) Number of spindles found at each T_{ngc} threshold bin. Vertical orange line indicates optimal performance of $T_{ngc} = 0.4$. (f) Cumulative number of spindles over the T_{ngc} range. Horizontal orange line indicates that the non-expert group identified 1669 spindles at $T_{ngc} = 0.4$. (g) By-subject correlation between spindle density in the gold standard and spindle density of the non-expert group consensus ($T_{ngc} = 0.4$). Each datapoint is one sleeping subject; darker circles indicate multiple subjects at the same position in the plot.
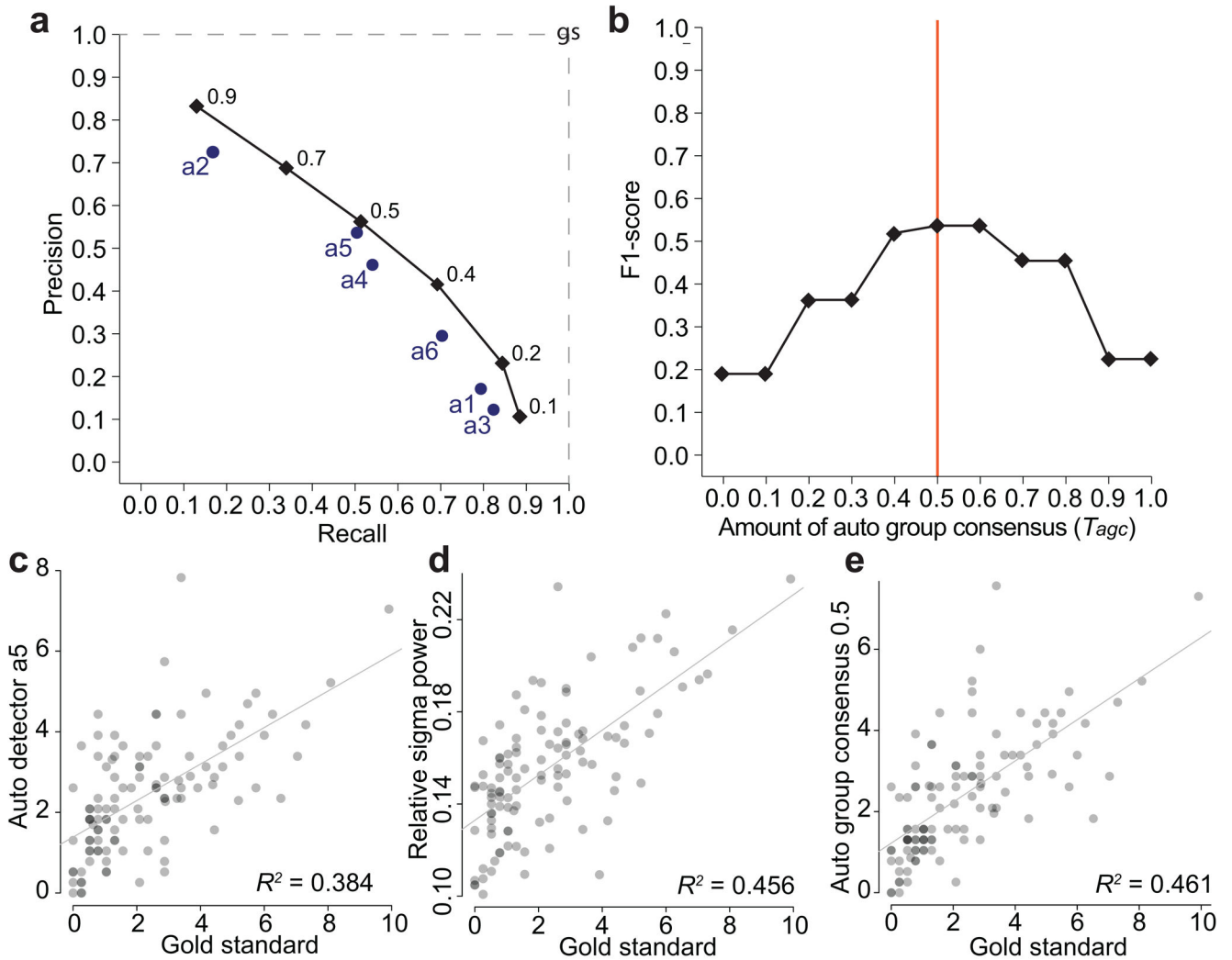
Figure 4.
Automated spindle detector performance. (a) Precision-recall plot of 6 automated detectors (indicated by 'a1'–'a6' text) and the automated group consensus curve (black line, labeled 0.1–0.9) at different levels of consensus. (b) F_1-score of the automated group consensus at different levels of consensus. Maximum performance was at $T_{agc} = 0.5$. Spindle density correlation between the gold standard density ($T_{egc} = 0.25$) and auto detector a5 density estimate (c), relative sigma power of the same segments of N2 sleep (d), or the auto group consensus density estimate ($T_{agc} = 0.5$, e). Each datapoint is one subject, darker points indicate multiple subjects at the same position in the plot.
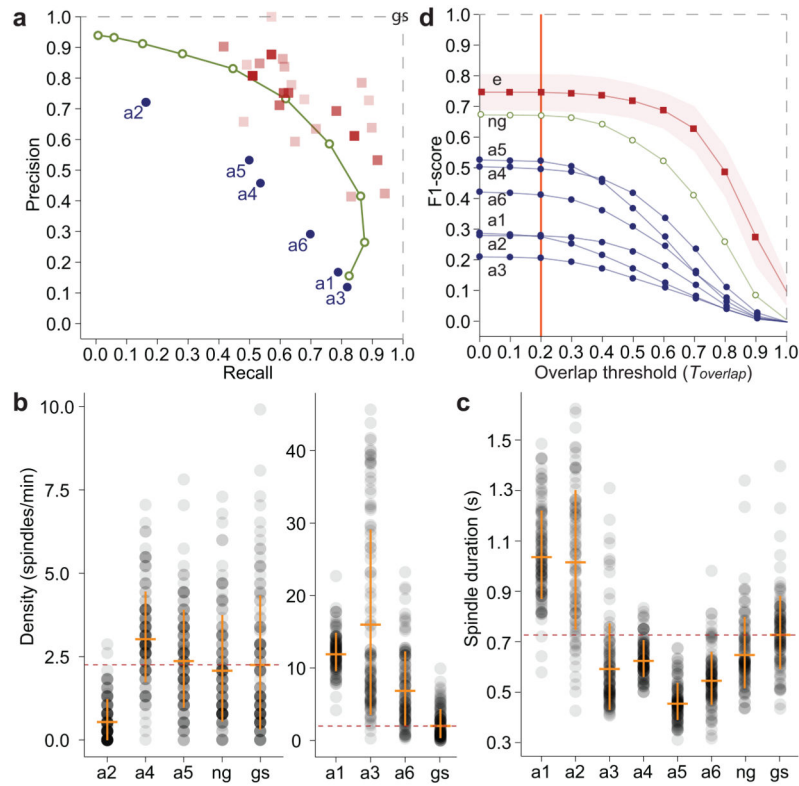
Figure 5.
Performance of experts, non-experts and automated spindle detection algorithms. (a) Precision-recall plot of experts (red boxes, after correction with the leave-one-out analysis), non-expert group (T_{ngc} = 0.0–0.9, green circles, also see Fig. 3) and automated methods (a1-a6) in the by-event analysis. Highest performance is closest to the top-right corner of the plot. (b) By-subject density estimates for each of the automated methods (a1-a6) and the non-expert group (ng) against the gold standard (gs). Each dot is one subject. Dotted line is the mean density in the gold standard. The mean and standard deviation of each detector is indicated by orange horizontal and vertical lines respectively. (c) By-subject spindle duration estimates; dotted line is the mean spindle duration in the gold standard. (d) The effect of varying the required amount of overlap ($T_{overlap}$) between event and detection in order to be determined a true positive on the performance of the automated detector (a1-a6), non-expert group (ng, n=114, at ngc = 0.4) or the mean individual expert (e, n=24, red shading is standard deviation). Vertical orange line indicates the $T_{overlap}$ threshold used by default in this study (0.2).

Table 1

Inter-detector by-event agreement, measured by F_1-score. (gs - gold standard ($T_{egc} = 0.25$), ngc - non-expert group consensus ($T_{ngc} = 0.4$), agc - automated group consensus ($T_{agc} = 0.5$).

	gs	ngc	agc	a1	a2	a3	a4	a5	a6
gs	1								
ngc	0.67	1							
agc	0.54	0.50	1						
a1	0.28	0.22	0.28	1					
a2	0.28	0.30	0.40	0.09	1				
a3	0.21	0.17	0.21	0.44	0.06	1			
a4	0.50	0.46	0.79	0.31	0.32	0.26	1		
a5	0.52	0.49	0.84	0.27	0.36	0.21	0.71	1	
a6	0.41	0.37	0.48	0.39	0.17	0.34	0.48	0.44	1